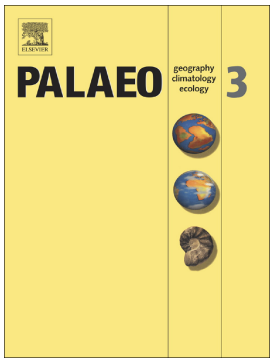

Linking glacier extent and summer temperature in NE Russia - Implications for precipitation during the global Last Glacial Maximum

Vera D. Meyer, Iestyn D. Barr

PII: S0031-0182(16)30920-8
DOI: doi: 10.1016/j.palaeo.2016.12.038
Reference: PALAEO 8126

To appear in: *Palaeogeography, Palaeoclimatology, Palaeoecology*

Received date: 4 July 2016
Revised date: 19 December 2016
Accepted date: 21 December 2016

Please cite this article as: Vera D. Meyer, Iestyn D. Barr , Linking glacier extent and summer temperature in NE Russia - Implications for precipitation during the global Last Glacial Maximum. The address for the corresponding author was captured as affiliation for all authors. Please check if appropriate. Palaeo(2016), doi: 10.1016/j.palaeo.2016.12.038

Linking glacier extent and summer temperature in NE Russia - implications for precipitation during the global Last Glacial Maximum

Vera D. Meyer[1,2] and Iestyn D. Barr[3]

1 Alfred-Wegener-Institute, Helmholtz Centre for Polar and Marine Research, Bremerhaven, Germany

2 Department of Geosciences University of Bremen, Germany

3 School of Natural and Built Environment, Queen's University Belfast, UK

Corresponding author: vera.meyer@awi.de

Abstract

It is generally assumed that during the global Last Glacial Maximum (gLGM, i.e. 18-24 ka BP) dry climatic conditions in NE Russia inhibited the growth of large ice caps and restricted glaciers to mountain ranges. However, recent evidence has been found to suggest that glacial summers in NE Russia were as warm as at present while glaciers were more extensive than today. As a result, we hypothesize that precipitation must have been relatively high in order to compensate for the high summer temperatures and the resulting glacial ablation. We estimate precipitation abundance by mass balance calculations for the paleo-glaciers on Kamchatka and in the Kankaren Range using a degree-day-modelling (DDM) approach, and find that precipitation during the gLGM was likely comparable to, or even exceeded, the modern average. We suggest that stronger than present southerly winds over the Northwest Pacific may have accounted for the abundant precipitation. The DDM-results imply that summer temperature, rather than aridity, limited glacier extent in the southern Pacific Sector of NE Russia during the gLGM.

Keywords: Siberia, Last Glacial Maximum, glaciation, precipitation, summer temperature

1) Introduction

An understanding of the extent of glaciers in East Asia during the global Last Glacial Maximum (gLGM, i.e. 18-24 ka BP, Mix et al. (2001)), and an appreciation of the underlying controlling mechanisms are important for the paleoclimate modelling community, as the presence of large ice-caps during this period would strongly impact climatic conditions in the North Pacific (N Pacific) region (Felzer et al., 2001, Bigg et al., 2008). Glacier extent in Northeast Russia (NE Russia) during the gLGM has been controversially discussed in the literature. For a long time the idea that a large pan-Arctic ice sheet stretched over western Beringia (Beringia is defined as the region stretching from Siberia to Alaska) dominated the scientific debate (Grosswald, 1988, 1998; Grosswald and Hughes, 2002; Grosswald and Hughes, 2005). However, this hypothesis was challenged by many studies in which Pleistocene moraines in NE Russia were dated using luminescence, cosmogenic and radiocarbon techniques. These studies provided evidence that Beringia remained largely ice-free during the gLGM, and that glaciers were restricted to mountain ranges (Velichko et al., 1984; Arkhipov et al., 1986; Glushkova, 2001; Gualtieri et al., 2000; Gualtieri et al., 2003; Brigham-Grette et al., 2003; Zamoruyev, 2004; Stauch and Gualtieri, 2008; Barr and Clark, 2012). For example, evidence was found to suggest that glaciers along the Pacific coast (e.g., in the Koryak Range and Kamchatka, Fig. 1A) were less than 80 km in length, and further inland (e.g., in the Pekulney Mountains) glaciers were even smaller, reaching a maximal length of ~ 40 km (Barr and Clark, 2012 and references therein). By now, the idea of limited mountain glaciation has become widely accepted, and it is generally supposed that the Beringian climate was too dry to allow extensive ice sheet growth during the gLGM (e.g. Brigham-Grette et al., 2003). Interestingly, several proxy-based paleoclimate studies (based on pollen, beetles and biomarkers) indicate that in Siberia, and in parts of the formerly exposed Bering Land Bridge (BLB), gLGM summers were as warm as, or even warmer than,

present (Elias, 2001; Alfimov and Berman, 2001; Kienast et al., 2005; Sher et al., 2005; Berman et al., 2011; Meyer et al., 2016a). This applies to many areas, including Kamchatka, a mountainous Peninsula attached to Chukotka (south-eastern Siberia; Fig. 1A, B), and the Kankaren Range, situated north of the Koryak Range (Fig. 1; Berman et al., 2011; Meyer et al., 2016a). Glacier reconstructions from these regions suggest that the local LGM occurred c.40 ka BP, and that the extent of glaciation then diminished towards the gLGM (Stauch and Gualtieri, 2008; Barr and Clark, 2012; Barr and Solomina, 2014). During the gLGM specifically, glaciation was restricted to relatively small mountain ice masses (smaller than during earlier periods of the glacial cycle), but was more extensive than during the Holocene (St. John and Krissek, 1999, Bigg et al., 2008; Barr and Clark, 2011; Barr and Solomina, 2014). If warm summers accompanied this gLGM mountain-glaciation, annual precipitation was probably more abundant than hitherto assumed, so that snow accumulation could compensate for ablation during warm summers. If this was the case, glacial summer temperatures would have been an important limiting factor for ice-expansion in these areas during the gLGM. This would challenge the prevailing view that ice extent was limited by the region's aridity.

In this paper we test this hypothesis by estimating precipitation on Kamchatka and in the Kankaren area during the gLGM by performing mass-balance calculations for paleo-glaciers in the Sredinny (Kamchatka) and Kankaren Ranges (Fig. 1). This is conducted using a degree-day-modelling approach (DDM, e.g., Laumann and Reeh, 1993; Hughes and Braithwaite, 2008). These areas are the focus of our investigation, since they are locations where Barr and Clark (2011) produce chronologically and geomorphologically constrained reconstructions of gLGM glaciers.

2) Regional setting and climate

The climate in NE Russia is generally classified as strongly continental and characterized by warm summers, cold winters and severe aridity (Ivanov, 2002). A general gradient towards less extreme conditions exists from the interior towards the Pacific coast as the marine influence increases. Kamchatka and the Kankaren Range are part of the Pacific Sector (Fig. 1A) where the climate is milder and wetter than in central Siberia. The general climatic conditions in the Pacific Sector are controlled by the interplay of the major atmospheric pressure systems over the North Pacific and the East Asian Continent. The winter climate is mainly determined by the presence of the Aleutian Low over the N Pacific and the Siberian High over Siberia. This atmospheric configuration lets northerly winds predominate over East Siberia which bring cold, arctic air masses to Pacific NE Russia. In summer, the North Pacific High (NPH) develops over the N Pacific, together with the East Asian Low over the continent. Under such conditions, southerly winds drive warm and moist maritime air masses into the Pacific Sector (Mock et al., 1998; Shahgedanova et al., 2002; Yanase and Abe-Ouchi, 2007).

2.1.Kamchatka Peninsula/Sredinny Range

Kamchatka is bordered by the Sea of Okhotsk to the West, the Northwest Pacific (NW Pacific) to the Southeast and the Bering Sea to the East (Fig. 1 A). Its topography is characterized by strong variations in relief, with lowlands along the coast and in the interior (Central Kamchatka Depression, CKD), and two major mountain ranges, the Sredinny Range and the Eastern Range (Fig. 1B). The Sredinny Range reaches a maximal altitude of 3621 m above sea-level (a.s.l.). The general climate of Kamchatka is cold maritime with cool and wet summers and mild, snowy winters (Dirksen et al., 2013). Mean July and January temperatures for the entire Peninsula range from 10 to 15°C and from -8 to -26°C, respectively (Ivanov, 2002) (see Fig. 2). In the coastal areas, precipitation is abundant

throughout the year, e.g. 1010 mm yr^{-1} at Petropavlovsk climate station (52.99°N, 158.66°E; Fig. 1A and 2). In interior valleys, precipitation is lower (~ 300 mm yr^{-1}) as the Mountain Ranges shield the marine influences. Klyuchi climate station (56.32°N, 160.83°E, Fig. 1A) notes average precipitation of 635 mm yr^{-1} (Fig. 2) but values as low as ~ 300 mm yr^{-1} have been reported for the CKD (Ivanov, 2002; Dirksen et al., 2013). Precipitation is highest in the mountain ranges where values typically vary between 1200 mm yr^{-1} and 1500 mm yr^{-1} (Ivanov, 2002; Dirksen et al., 2013).

Today, small glaciers are only present on the highest peaks (Solomina and Calkin, 2003; Ananicheva et al., 2008; Lynch et al., 2016). A glacier reconstruction by Barr and Clark (2011) suggests that during the gLGM a continuous, mountain-centred ice field existed in the Sredinny Mountains (Fig. 1B). Its outlet glaciers extended up to 80 km into surrounding valleys, and the ice-field covered 57,363 km^2 (Barr and Clark, 2011). End-moraines of potential gLGM age also exist in the Eastern Range. However, since accurate dates to clearly ascribe these Eastern Range moraines to the gLGM are missing (Barr and Solomina, 2014), this paper focusses on the Sredinny Range, rather than Kamchatka as a whole.

2.2.The Kankaren Range and adjacent lowlands

The Kankaren Range is attached to the northern flanks of the Koryak Range and faces the Anadyr-Lowlands (AL) in the North (Fig. 1A). The Kankaren Mountains reach maximal altitudes of 1200 m a.s.l.. Direct observations of modern climate conditions in the mountains themselves are lacking. The closest climate stations are in Alkatvaam (63.133°N, 179.03°E) and Meynypilgyno (62.54°N, 177.05°E; Fig. 1A), respectively, ~ 60 km East, and ~ 85 km South of the Kankaren Mountains, where average July, January and annual temperatures (10.8°C, -15.7°C and -5.2°C) are typically lower than on Kamchatka (see Fig. 2).

Precipitation values for the Kankaren Range are also lacking, though the data from Alkatvaam and Meynypilgyno suggest modern precipitation of ~ 439 mm yr^{-1} (http://de.climate-data.org). According to the glacier reconstruction by Barr and Clark (2011), the western part of the Kankaren Range was covered by a mountain-centred ice-field during the gLGM, while the eastern sector was occupied by a group of five valley glaciers (Fig. 1C). This reconstruction reveals glaciers up to 7 km in length and a total ice covered area of 215 km^2. By contrast, the mountains are currently glacier free.

3) Degree Day Modelling

3.1.General Model setup

In order to estimate the accumulation necessary to sustain the reconstructed gLGM glaciers in the Sredinny and Kankaren Ranges (reconstruction from Barr and Clark, 2011), given summer temperatures equivalent to modern, we applied a degree day modelling (DDM) approach – allowing the annual accumulation needed to balance annual ablation at the equilibrium line altitudes (ELAs) of former glaciers to be estimated (Laumann and Reeh, 1993; Braithwaite et al., 2006). A glacier's ELA is defined as the altitude where net annual accumulation and ablation are in equilibrium, and is largely controlled by climate (Ohmura et al., 1992). In the DDM approach, the annual melt at the glacier's ELA is calculated from the sum of daily melt values (M_d). Each M_d can be calculated as a function of daily mean temperature (where positive) at the paleo-ELA (T_d; eq. 1) and a degree-day melt factor (DDF; eq. 1). In this study DDFs of 4.0 and 2.5 mm d^{-1} $°C^{-1}$ are used (Braithwaite et al., 2006). The former is based on the assumption that gLGM glaciers were temperate (with high mass-flux), and the latter on the assumption that they were of polar type (with low mass-flux).

$$M_d = T_d * DDF \quad \text{(eq. 1)}$$

The annual sum of these daily melt values is then assumed to be equalled by accumulation (expressed in mm) at the ELA (since, at the ELA, annual accumulation = annual ablation).

Assuming that the annual distribution of temperatures is described by a sine curve, (Brugger, 2006; Hughes, 2008, 2009; Hughes and Braithwaite, 2008) daily temperatures at the paleo-ELA can be calculated from mean annual air temperature at the paleo-ELA as follows (eq. 2):

$$T_d = A_y \sin\left(\frac{2\pi d}{\lambda} - \square\right) + T_a \quad \text{(eq. 2)},$$

where A_y is the amplitude of annual temperature variability (1/2 of the annual temperature range), d the ordinal day, λ is the period (365 days), ϕ is the phase angle of the sine curve (here 1.93 radians based on the general assumption that temperature is maximal in July and minimal in January), and T_a is mean annual air temperature.

3.2.Setup of simulated scenarios for Kamchatka and in the Kankaren Range

In order to estimate the gLGM accumulation for the Sredinny and the Kankaren mountain ranges, the DDM was applied to paleo-ELA data from Barr and Clark (2011). For the Sredinny Range, the model was run with the mean ELA of the entire Sredinny ice-field and with average ELAs of the southern, central and northern sectors of the ice field (Fig. 1B). The division was implemented as the ELA-reconstruction by Barr and Clark (2011) yielded a north-south gradient with a decrease in ELAs towards the north. In the Kankaren Range, an ELA gradient was not reconstructed rendering a separation into sectors not necessary. The DDM was applied only to the mean ELA of the entire glacier-field (Fig. 1C). gLGM conditions were simulated assuming that glacial mean July temperatures (T_{July}) equal modern values (Alfimov and Berman, 2001; Berman et al., 2011; Meyer et al., 2016a), but winters were colder than at present (Meyer et al., 2002), conditions yielding a larger A_y compared to today.

In order to simulate LGM temperatures (T_d, eq. 2) for the Sredinny and Kankaren ranges, the perturbation in mean annual temperature during the gLGM relative to pre-industrial conditions ($\Delta T_{a\ LGM}$) was calculated from climate-model data (Kim et al., 2008) since, to our knowledge, no proxy-based absolute estimates of mean annual temperature during the gLGM exist for the Kankaren or Sredinny Ranges. For eastern Siberia as a whole, the climate-model suggests a $\Delta T_{a\ LGM}$ of ~ 6-14°C (Kim et al., 2008). If T_{July} during the gLGM is known (assumed to equal modern), A_y at the LGM (A_{yLGM} needed to calculate daily temperatures, eq. 2) can be approximated by eq. 3 (again, assuming that the annual distribution of temperatures is described by a sine curve with July and January being the warmest and coldest months of the year):

$$A_y = T_{July} - T_a \quad \text{(eq. 3)}$$

Modern T_{July} and T_a for Kamchatka were calculated by combining data from Klyuchi and Petropavlovsk climate stations (Fig. 1A and 2). The stations represent the continental climate of the CKD and the maritime conditions at the Eastern Coast (http://en.climate-data.org)—the areas most relevant to palaeotemperature reconstructions from Meyer et al. (2016a). The averaged data from these two climate stations indicate modern July, January and annual temperatures of 13.1°C, -12.0°C, and 0.4°C, respectively (see Fig. 2). Correcting these data for altitude, using a lapse-rate of 0.63°C/100 m (Osipov, 2004), gives a modern sea level T_{July} and T_a of 13.2°C and 0.6°C, respectively, and an A_y of 12.6°C (based on mean monthly values) (see Fig. 2 and Table 1). Modern T_{July} and T_a for the Kankaren Range were calculated by combining data from Alkatvaam and Meynypilgyno climate stations (Fig. 1A). Correcting these data for altitude reveals modern sea level T_{July} and T_a values of 10.9°C and -5.1°C, respectively (see Fig. 2 and Table 1).

In the present study, given the $\Delta T_{a\ LGM}$ range of -6 to -14°C predicted by the climate model of Kim et al. (2008), we considered gLGM climate scenarios for both the minimal and maximal $\Delta T_{a\ LGM}$ estimates (see Table 2). In addition, as the modern temperature data reflect the conditions at sea-level, T_a was lowered using a lapse-rate of 0.63°C/100 m (Osipov, 2004) in order to obtain air temperature data at the paleo-ELAs of the gLGM glaciers reconstructed by Barr and Clark (2011) (see Tables 2 and 3). DDM-derived estimates for gLGM precipitation are given as absolute values in mm yr^{-1} and in percentage relative to modern using the range of 1200-1500 mm yr^{-1} (Ivanov, 2002; Dirksen et al., 2013).

4. Results

4.1. Simulated summer and winter temperature at the gLGM

Given that the model runs are based on modern T_{July}, but enforce a 6 to 14°C reduction in mean T_a, $A_{y\ LGM}$ increases correspondingly (see eq. 3 and Fig. 3). In order to keep T_{July} at modern values, $A_{y\ LGM}$ increases in equal but inverse value with $\Delta T_{a\ LGM}$ (as it decreases). As a result, at the mean ELA of the Sredinny ice field, $A_{y\ LGM}$ varies from 18.6°C to 26.6°C, based on $\Delta T_{a\ LGM}$ values of -6°C and -14°C, respectively (see Fig. 3). This results in mean January temperatures ($T_{Jan.}$) as low as -29.5°C and -45.5°C during the gLGM (12°C and 28°C below modern values) (Fig. 3A). Similarly, in the Kankaren Range, $A_{y\ LGM}$ varies from 22.0°C to 30.0°C, based on $\Delta T_{a\ LGM}$ values of -6°C and -14°C, respectively (see Fig. 3), resulting in mean $T_{Jan.}$ of -31.2°C and -47.2°C during the gLGM (12°C and 28°C below modern values) (Fig. 3B). In the Sredinny as well the Kankaran Range the number of positive degree days obtained for the gLGM using both $\Delta T_{a\ LGM}$ values of -6°C and -14°C, is smaller than at present. $\Delta T_{a\ LGM}$ of -14°C yields the fewest positive degree days (Fig. 3).

4.2. Annual accumulation/precipitation

The DDM-derived estimates of total annual accumulation and the duration of the ablation season (days with positive degree days) given $\Delta T_{a\ LGM}$ values of -6 and -14°C for temperate glaciers (DDF of 4.0) are shown in Table 2 and for glaciers of polar type (DDF of 2.5) in Table 3. It is worth noting that these estimates of annual accumulation do not represent direct estimates of former annual precipitation, since the latter also includes precipitation (likely falling as rain) during the ablation/summer season (not included in the output of the DDM). However, since the gLGM ablation season in each of our scenarios is relatively short (ranging between 71 and 113 days; see Tables 2 and 3), and because the DDM model fails to account for the contribution of accumulating snow and ice from non-direct sources (i.e., windblown and/or avalanched snow and ice from the surrounding landscape), which can be significant in some cases (see Kern and László, 2010), the accumulation estimates derived here are regarded as rough estimates of annual precipitation.

4.2.1. Sredinny Range

Modelled estimates of gLGM precipitation in the Sredinny Range based on a $\Delta T_{a\ LGM}$ of -14°C (1479-1986 mm yr^{-1}) are always lower than their equivalents based on a $\Delta T_{a\ LGM}$ of -6°C (1780-2394 mm yr^{-1}; see Tables 2 and 3, Fig. 3). Precipitation is always higher for temperate glaciers (1479-2394 mm yr^{-1}, see Table 2) than for glaciers of polar type (924-1496 mm yr^{-1}, see Table 3). Assuming temperate glaciers (DDF of 4.0), the model output suggests that 1780–2145 mm yr^{-1} of precipitation would be necessary to sustain the mean ELA of the entire Sredinny ice field (897 m.a.s.l.), considering both $\Delta T_{a\ LGM}$ values. When compared to modern precipitation values in the mountains this constitutes a 19–79% increase in annual precipitation (Table 2). For both $\Delta T_{a\ LGM}$ values, the average ELA of the southern sector of the Sredinny ice field requires the lowest precipitation (1479–1780 mm yr^{-1}). Values

are intermediate in the central sector (1829–2203 mm yr^{-1}), and greatest in the northern part of the ice-field (1986–2394 mm yr^{-1}).

These trends are also apparent when polar-type glaciers are assumed (DDF of 2.5, Table 3), since the model suggests that 1113–1340 mm yr^{-1} of precipitation would be necessary to sustain the mean ELA of the entire Sredinny ice field (897 m.a.s.l), constituting between a ~ 26% decrease and ~ 12% increase relative to present (Table 3, Fig. 3). Precipitation is lowest for the average ELA of the southern sector of the Sredinny ice field (924–1112 mm yr^{-1}), values are again intermediate in the central sector (1143–1377 mm yr^{-1}), and the ELAs of the northern sector require the greatest precipitation to sustain the glaciers in equilibrium (1241–1496 mm yr^{-1}).

Considering all scenarios, maximal precipitation (2394 mm yr^{-1}) is found for the combination of temperate glaciers, milder winters ($\Delta T_{a\ LGM}$ of -6°C) and an ELA of 808 (northern part of the ice field, Table 1). Minimal precipitation (924 mm yr^{-1}) estimates are found in the southern sector (ELA of 1035) when colder winters and glaciers of polar type are assumed (Table 3).

4.2.3. Kankaren Range

In the Kankaren Range the average ELA at the gLGM was 575 m (a.s.l) according to Barr and Clark (2011). Given this value, the precipitation required to keep the glaciers in equilibrium ranges between 589 and 1291 mm yr^{-1} considering all scenarios (different ΔT_a and glacier types). In all scenarios, gLGM precipitation estimates are lower than in their equivalents for the Sredinny Range (see Tables 2 and 3).

Like in Kamchatka, estimates for gLGM precipitation assuming colder winters ($\Delta T_{a\ LGM}$ of -14°C; i.e. 589-943 mm yr^{-1}, see Tables 2 and 3) are lower than in the scenarios based on a $\Delta T_{a\ LGM}$ of -6°C (807-1291 mm yr^{-1}, Tables 2 and 3). Also, assuming glaciers of polar type

(DDF of 2.5 mm d^{-1} $°C^{-1}$, Table 3), the precipitation required to keep the gLGM glaciers in equilibrium (i.e. 589–807 mm yr^{-1}) is lower than for temperate glaciers (i.e. 943-1291 mm yr^{-1}), the same tendency found for the Sredinny Range.

Again, maximal precipitation is found when warm winters and temperate glaciers are assumed (1291 mm yr^{-1}, Tables 2 and 3) while the combination of cold winters and glaciers of polar type requires the lowest precipitation to sustain the gLGM glaciers (589 mm yr^{-1}, Tables 2 and 3).

5. Discussion

5.1. Inferences for gLGM precipitation

If gLGM glaciers in Kamchatka are assumed to have been temperate (with a DDF of 4.0 mm d^{-1} $°C^{-1}$), model scenarios generally suggest increased mean annual precipitation at the gLGM relative to modern conditions (with estimates suggesting a change of between +18.7% to +99.5% relative to modern values; see Table 2). The southern sector of the Sredinny ice-field, where ELA is highest, is an exception when $\Delta T_{a\ LGM}$ of -14°C, and hence colder winters, are assumed, as the modelled value (i.e. 1479 mm yr^{-1}) is slightly lower than 1500 mm yr^{-1} (Table 2) suggesting precipitation equalled the modern mean.

If glaciers are assumed to have been of polar type (i.e., with a DDF of 2.5 mm d^{-1} $°C^{-1}$), then less mean annual precipitation than for temperate glaciers is needed to sustain the glaciers at the gLGM. Precipitation is similar to modern values as the majority of the estimates for the central and northern Sredinny ice field adopted from the DDM fall in the range of modern precipitation (1200-1500 mm yr^{-1}, see Table 3). The two scenarios assuming polar-type

glaciers in the southern sector yield values below the modern range. When $\Delta T_{a\ LGM}$ of- 6°C is assumed (i.e. relatively warm winters) precipitation (1113 mm yr^{-1}) is slightly below the low end of the modern range (1200 mm yr^{-1}), It is even reduced by ~ 23 to ~ 38% (924 mm yr^{-1}), relative to present, for $\Delta T_{a\ LGM}$ of -14°C (relatively cold winters). In the central part of the ice field (ELA 808 m a.s.l.) precipitation (1143 mm yr^{-1}; Table 3) is reduced relative to present, though very close to the lower end of the modern range (1200 mm yr^{-1}). This indicates that in combination with polar-type glaciers severe winters (T_{Jan} of -45.5°C at mean ELA; $A_{y\ LGM}$ of 26.6 °C) may have allowed glaciers of the southern Sredinny ice field to be in equilibrium conditions when precipitation was significantly (>10% relative to 1200 mm yr^{-1}) reduced relative to present while summers were as warm as today. In the central and northern part of Sredinny ice field because gLGM precipitation must have equalled modern values, despite reduced winter temperatures.

In the Kankaren Range the model suggests gLGM precipitation exceeds the modern value averaged from Alkatvaam and Meynypilgyno climate stations (~ 439 mm yr^{-1}) by about 34-194%. However, these lowland stations are not representative of mountain conditions, as precipitation usually increases with altitude. So, the lack of robust information about modern precipitation in the Kankaren Range prevents direct comparison with modern values in the mountains. However, the difference between our estimates for gLGM precipitation in the Sredinny and Kankaren ranges (~ 500 mm yr^{-1}) is similar to the modern deviation between averaged values for Alkatvaam and Meynypilgyno climate stations (~ 439 mm yr^{-1}) and the value compiled from Klyuchi and Petropawlowsk (~823 mm yr^{-1}). Considering this, the DDM results imply that sign and magnitude of gLGM-to-Holocene precipitation changes may have been similar in both areas (i.e., in the Sredinny and Kankaren ranges).

In conclusion, our model results imply that irrespective of the annual temperature range ($\Delta T_{a\ LGM}$ i.e. a reduction in winter temperature) or glacier type (DDF) used, annual precipitation in

Pacific Russia during the gLGM must have been similar to, or even exceeded, modern values if summers were as warm as present while mountain glaciers were more extensive than today (reaching the sizes suggested by Barr and Clark, 2011).

5.2. Comparison with proxy data

Unfortunately, an assessment of whether precipitation on Kamchatka during the gLGM was similar to, or even greater than, today cannot be made on the basis of independent proxy-data, since such information is not available (Dirksen et al., 2013). In the Kankaren Range, pollen-based climate reconstructions provide evidence for the former presence of snow-bed plant-communities thereby indicating abundant snow-accumulation during the gLGM (Lozhkin and Anderson, 2013; Anderson and Lozhkin, 2015), a finding generally in concert with the presence of glaciers and abundant precipitation. On the other hand, pollen assemblages also contrast with our findings, as the paucity of shrubs in the Kankaren region points to reduced moisture availability, relative to today (Lozhkin and Anderson, 2013; Anderson and Lozhkin, 2015). One possibility to explain discrepancies between DDM results and the pollen-interpretation is that aridity persisted in the Kankaren Range at the gLGM, despite increased precipitation, as moisture may have been trapped in glaciers and ground ice (Sergin and Scheglova, 1976; Alfimov and Berman, 2001), meaning that precipitation, even if abundant, may not have been available to plants.

Nevertheless, there are good environmental reasons to expect increased aridity through reduced precipitation in the Siberian interior as well as along the Pacific coast during the gLGM. For example, he growth of ice-sheets elsewhere in the Northern Hemisphere is presumed to have deprived NE Russia of moisture (e.g. Seigert et al., 2001; Stauch and Gualtieri, 2008).Moreover, during this period, the Bering and Chukchi-Shelves were exposed, reducing marine influences in western and central Beringia (Laukhin et al., 2006;

Yanase and Abe-Ouchi, 2007; Barr and Clark et al., 2011). In addition, proxy-based studies point to extensive sea-ice coverage (Sakamoto et al., 2005; Caissie et al., 2010; Smirnova et al., 2014) which also suggests that winter sea surface temperatures were lower than at present. These factors would reduce evaporation over the marginal N-Pacific (Sancetta, 1983) and are supported by paleoclimate modelling studies which find no indication of increased precipitation in the N Pacific realm during the gLGM (Yanase and Abe-Ouchi, 2007), but do indicate reduced annual precipitation (by ~ 30–60%; Budiko et al., 1992; Velichko, 1993; Yanase and Abe-Ouchi, 2007). Also, further north in the Pacific Sector (Anadyr Lowlands; area of Pekulney Mountains, Fig. 1A) as well as in the non-Pacific Sector (Fig. 1A), pollen point to increased aridity during the gLGM (Sher et al., 2005; Kienast et al., 2005; Lozhkin et al., 2007; Andreev et al., 2011; Lozhkin and Anderson, 2013). It therefore appears that existing paleo-environmental indicators generate a palaeoclimatic scenario for the NW Pacific realm, whereby extensive mountain glaciation, warm summers and arid conditions coexisted. This contrasts the findings from the DDM. The disagreement between the DDM results and climate indicators from the Siberian North may be explained by a strong precipitation gradient with wet conditions along the coast and very dry conditions in the interior. Such a gradient is reflected by the gLGM glacier extent in Siberian Mountain Ranges, as Barr and Clark (2012) noted that during the gLGM glaciers were largest in the coastal areas (i.e. Kamchatka and the Koryak Range) and became smaller in mountain ranges further inland (e.g. Anyuy and Pekulney Mountains). The Verkhoyansk Mountains (centred on ~ 67°N, 127°E) even appear to have remained largely ice free during the gLGM (Stauch and Gualtieri, 2008; Stauch and Lehmkuhl, 2010; Zech et al., 2011; Barr and Clark, 2012). Furthermore, palaeobotanical evidence indicates that Beringia was a mosaic of different vegetation regimes during the gLGM (e.g. Elias and Crocker, 2008; Kuzmina et al., 2011 Anderson and Lozhkin, 2015 and references therein), and this may reflect a variety of climate

zones that vary with respect to temperature and moisture. However, concerning the Pacific Sector of Siberia, this picture consisting of warm summers, reduced precipitation and extensive mountain glaciation appears to contradict inferences made from the DDM approach adopted here. As such, the assertion that extensive glaciers and warm summer temperatures coincided in Pacific NE Russia at the gLGM may be brought into question.

Uncertainties in the chronologies of either temperature or glaciation proxies may explain the discrepancies; yet the chronology for the marine sediment-core (dated by ^{14}C of planktic foraminifera and by core-to-core correlations of XRF data from a set of sediment cores obtained from the Bering Sea and the NW Pacific) on which the temperature record for Kamchatka was established accurately defines the gLGM (Max et al., 2012; Meyer et al., 2016a, b). Also, studies which indicate that in western Beringia and the on the BLB summers during the gLGM were as warm as (or even warmer than) today, are based on soil sequences in which the gLGM is well constrained by radiocarbon dating of plant remains, insects and mammal bones (Elias, 2001; Kienast et al., 2005; Sher et al., 2005). In terms of glaciation, a small number of radiocarbon dates from the Sredinny Mountains suggest deglaciation prior to 10-21 ka. When calibrated using the IntCal13 calibration curve (Reimer et al., 2013) and CALIB 7.1 program (Stuiver et al., 2016), this age range extends to 9.6-23.4 ka BP. On this basis, moraines in the Sredinny Mountains, and the glacier reconstruction of Barr and Clark (2011), are assigned to the gLGM (18-24 ka BP; Braitseva et al., 1968; Melekestsev et al., 1970; Stauch and Gualtieri, 2008; Barr and Clark, 2016). Similarly, cosmogenic dating (^{36}Cl) from the Koryak and Kankaren Ranges suggest exposure (i.e., deglaciation) between 10.62 and 21.65 ka, again constraining the glacier reconstruction of Barr and Clark (2011) to the gLGM (i.e. 18-24 ka BP). Though online tools allow ^{36}Cl ages to be re-calibrated (e.g., CRONUScalc; Marrero et al., 2016), this procedure relies on the original reporting of detailed methodological and laboratory information (e.g. latitude, longitude, elevation,

sample thickness, sample density, topographic shielding correction factor, CN production rates, scaling factors) (Small et al., 2016). Without this information legacy data cannot be updated to reflect the current state of knowledge and its overall reliability is ambiguous (cf. Small et al. 2016). Unfortunately, for the Gualtieri et al. (2000) data, the required information is unavailable, and we therefore report ^{36}Cl ages as originally published (e.g., Small et al., 2016) while acknowledging that any inferences drawn must be treated with appropriate caution. Fortunately, a supporting chronology for the terrestrial ^{14}C and ^{36}Cl ages is provided by sediment cores from the NW Pacific which indicate that ice rafted debris (IRD), originating from the Kamchatka Peninsula (St John and Krissek, 1999), was continuously deposited throughout Marine Isotope Stage (MIS 2; i.e. 14-29 ka BP) and only ceased c.14-15 ka BP (St. John and Krissek, 1999; Kiefer et al., 2001; Bigg et al., 2008; Gebhardt et al., 2008). In these records, the gLGM is well constrained by radiocarbon dated foraminifera (e.g Kiefer et al., 2001; Gebhardt et al., 2008). Thus, the IRD records suggest that outlet glaciers from the eastern coast of Kamchatka terminated in the NW Pacific during the gLGM and that ice retreat did not occur until c.15 ka BP. This supports the terrestrial chronology, which suggests that the reconstruction of Barr and Clark (2011) (Fig. 1B) represents ice extent at the gLGM (18-24 ka BP). As a consequence, the coexistence of warm summers and extensive mountain glaciation at the gLGM is considered likely and uncertainties in either the glacial or the temperature chronology fail to fully account for the discrepancies between several environmental indicators noted in this paper. Hence, the view of abundant precipitation in the Pacific Sector of Siberia during the gLGM is supported.

5.3. Possible mechanisms for abundant annual precipitation at the gLGM

Meyer et al. (2016a) suggested that the warm summers on Kamchatka resulted from stronger-than-present southerly winds over the subarctic NW Pacific due to a strengthening, or

westward displacement, of the NPH. Besides summer warming, increased advection of maritime air masses from the south simultaneously leads to more precipitation during the summer months in southeast Siberia, as summarized in the climate synopsis for Beringia by Mock et al. (1998). Given this interpretation, the temperature record may be an indirect indication for wetter-than-present conditions in Pacific Siberia during the summer season. Unfortunately, no direct proxy-based reconstructions of gLGM precipitation are available, so this assumption remains to be tested. Increased precipitation in the summer months contrasts with several studies utilising General Circulation Models, which predict that summer precipitation in East Asia was significantly reduced during the gLGM (Yanase and Abe-Ouchi, 2007). To explain this reduction, Yanase and Abe-Ouchi (2007) suggested two underlying mechanisms: (I) weakened advection of maritime air masses to the East Asian coast in response to a weakened NPH. (II) A reduction of precipitable moisture as a consequence of reduced evaporation over the NW Pacific due to lowered SST. (I) can be challenged by the proxy-based inference for increased southerly flow over Kamchatka (Meyer et al. 2016a). However, (II) seems to be a robust scenario since various SST records from the open North Pacific (south of 50°N) show lowered temperature during the LGM (e.g. Harada et al., 2012). However, in the marginal NW Pacific, in the vicinity of Kamchatka (site 12KL, Fig. 1A), summer SST during the LGM was probably only 1°C lower than at present (Meyer et al., 2016b), thereby giving reason to assume the NW Pacific was free of sea ice during LGM summers. Given relatively warm SST and limited sea-ice extent, evaporation over the subarctic NW Pacific may not have differed significantly from present. Considering alkenone-based SST records, the same may have applied for the Sea of Okhotsk, since these records suggest that glacial temperatures in the area were similar to present (Seki et al., 2004; Harada et al., 2012). However, these records are assumed to be biased by shifting production-seasons of the alkenone-producing coccolithophores (e.g. Seki et al., 2004, 2009), a

hypothesis which is supported by SST reconstructions based on TEX^{L}_{86}-paleothermometry which indicate a cooling of ~ 5°C relative to modern (Harada et al., 2012; Seki et al., 2014). Nevertheless, in the subarctic NW Pacific, minor changes in evaporation (between gLGM and present) combined with increased southerly winds during the summer months may have resulted in abundant precipitation in the Pacific sector of Siberia at the gLGM.

5.4. Implications for glacier growth in NE Russia at the gLGM

The conclusions of chapter 5.3 suggest that summer precipitation may have mainly accounted for the precipitation necessary to sustain glaciers in the Pacific Sector during the gLGM. As noted in section 4, results from the DDM do not directly include precipitation during the ablation season, as this is presumed to largely fall as rain at the ELA (and therefore not contribute to glacial accumulation). However, it is possible that precipitation above the ELA fell as snow even during summer months, and thereby contributed to the glacier growth. Additional, the ablation season (number of positive degree days) was likely shorter than today, as suggested by our simulations for the annual temperature cycle during the gLGM (see Fig. 3). A short ablation season may have supported glacier stability by limiting total annual ablation. Also, colder winters in combination with polar-type glaciers explain why glaciers were more extensive than today while at the gLGM precipitation and summer temperature were similar than at present.

By indicating that annual precipitation in Pacific Russia during the gLGM must have been as abundant as today or even exceeded the modern values if summers were as warm as present while mountain glaciers were more extensive than today, the DDM-results from the present study suggest that warm summer temperatures limited gLGM glacier growth in south-eastern Pacific Siberia. Interestingly, DDM-derived estimates for glacial precipitation in the Pekulney Mountains (north of the Anadyr-Lowlands, 66.09°N, 175.10°E, Fig. 1A) from Barr

and Clark (2011) suggest that precipitation must have exceeded modern values, although gLGM summer temperature was estimated to have been 3.1-4.1°C lower than at present (Alfimov and Berman, 2001; Barr and Clark, 2011). This finding suggests that also in the north-eastern Pacific Sector summer temperature may have limited glacier growth. However, Barr and Clark (2011) acknowledged that gLGM temperature reconstructions for the Pekulney area vary considerably (Alfimov and Berman, 2001; Lozhkin et al., 2007; Barr and Clark, 2011), and calculations based on a 6.4°C reduction in T_{July} (Lozhkin et al., 2007), would suggest that annual LGM accumulation was below the modern mean, supporting that aridity hampered glacier growth at the gLGM (Brigham-Grette et al., 2003; Stauch and Gualtieri, 2008; Barr and Clark, 2011; Barr and Spagnolo, 2013). Therefore, Barr and Clark (2011) considered the first scenario unlikely. In light of our findings, and with evidence for warm gLGM summers being widespread in Siberia (Alfimov and Berman, 2001; Elias, 2001; Kienast et al., 2005; Sher et al., 2005; Berman et al., 2011; Meyer et al., 2016 a), the relatively high precipitation estimates may now appear more likely. As such, and despite the ambiguity in the Pekulney Mountains, the DDM-derived precipitation estimates for the three mountain ranges (the Sredinny, Kankaren and Pekulney) emphasize that summer temperature may have been an important limiting factor for glacier growth in the Pacific Sector of Siberia at the gLGM. This contrasts with the prevailing view that glacier expansion in NE Russia was hampered by increased aridity (Seigert et al., 2001; Brigham-Grette et al., 2003; Stauch and Gualtieri, 2008; Barr and Clark, 2011; Barr and Spagnolo, 2013), at least regarding the Pacific Sector. Since proxies suggest that extreme arid conditions prevailed due to increased continentality in interior Siberia (e.g. Guthrie et al., 2001; Kienast et al., 2005; Sher et al., 2005; Lozhkin et al., 2007), the aridity hypothesis may apply to regions in continental Siberia.

6. Summary and Conclusion

There is consensus that the local LGM in NE Russia preceded the gLGM, occurring around 40 ka BP and that glaciers shrank towards the gLGM. At the gLGM glaciation was restricted to mountain glaciers in Siberian mountain ranges, such as the Sredinny (Kamchatka) and the Kankaren Range. Evidence exists to suggest that during the gLGM, summers in Kamchatka and the Kankaren Range were as warm as at present while mountain glaciation was more extensive than today. As a result, we hypothesized that, during this period, precipitation must have been abundant (at least comparable to present) and that summer temperature was an important limiting factor for ice-sheet growth in the Pacific Sector of NE Russia. Our DDM-results support this hypothesis indicating that despite a reduction in winter temperatures, annual precipitation at the gLGM, was similar to, or higher than the modern mean, depending on whether glaciers were of polar or temperate type. In the Pacific Sector precipitation may have been increased relative to today due to stronger southerly winds during the summer season and relatively warm SST in the marginal NW Pacific, and this may have resulted in heavy snowfall above the ELA, allowing glaciers to develop and persist despite warm summer temperatures. Additionally the ablation season may have been notably short, thereby limiting total ablation. However, the majority of paleo-environmental indicators from interior and Pacific Siberia as well as the subarctic N Pacific point to dryer-than-present conditions in continental Siberia and the Pacific Sector at the gLGM. This is why it is generally assumed that strong aridity restricted glaciation in NE Russia during the gLGM, an idea our findings are in contrast with. Discrepancies with interior Siberia may be due to pronounced regional differences in Beringian climate with wet conditions in maritime Siberia and severe dryness in farther inland. Thus, strong aridity potentially inhibited glacier growth in continental Siberia while summer temperature restricted glacier expansion in regions bordering the Pacific coast. Discrepancies in the Pacific Sector together with the sparseness of independent

proxy data for precipitation in this region highlight the need of further investigations of Beringian palaeo-climate through the last glacial cycle.

Acknowledgements

This study was conducted within the frame of a PhD-project which was funded by the by the Helmholtz association through the President's Initiative and Networking Fund. GLOMAR – Bremen Graduate School for Marine Sciences is thanked for funding V. Meyer's research stay at Queen's University Belfast which allowed the realization of the project. The staff of the department of Geography, Archaeology and Paleoecology at Queen's University Belfast are thanked for their kind support during the research stay. We are also grateful to Phil Hughes and Julie Brigham-Grette for their detailed and constructive reviews.

References

Alfimov, A.V., Berman, D.I., 2001. Beringian climate during the late Pleistocene and Holocene. Quat. Sci. Rev. 20, 127–134.

Ananicheva, M. D., Krenke, A. N., Hanna, E., 2008. Mountain glaciers of NE Asia in the near future: a projection based on climate-glacier systems interaction. Cryosphere Discussion, 2, 1-21.

Anderson, P. A., and Lozhkin, A. V., 2015. Late Quaternary vegetation of Chukotka (Northeast Russia), implications for Glacial and Holocene environments of Beringia. Quat. Sci. Rev. 107, 112-128.

Andreev, A. A., Schirrmeister, L., Tarasov, P. E., Ganopolski, A., Brovkin, V., Siegert, C., … Hubberten, H. W., 2011. Vegetation and climate history in the Laptev Sea region (Arctic Siberia) during Late Quaternary inferred from pollen records. Quat. Sci. Rev., 30, 2182–2199. http://doi.org/10.1016/j.quascirev.2010.12.026

Arkhipov, S.A., Isaeva, L.L., Bespaly, V.G., Glushkova, O.Y., 1986. Glaciation of Siberia and North-East USSR. Quat. Sci. Rev. 5, 463–474.

Barr, I.D., Clark, C.D., 2011. Glaciers and climate in Pacific Far NE Russia during the Last Glacial Maximum. J. Quat. Sci. 26, 227–237.

Barr, I.D., Clark, C.D., 2012. Late Quaternary glaciations in Far NE Russia: combining moraines, topography, and chronology to assess regional and global glaciation synchrony. Quat. Sci. Rev. 53, 72–87.

Barr, I.D., Solomina, O., 2014. Pleistocene and Holocene glacier fluctuations upon the Kamchatka Peninsula. Glob. Planet. Change, 1–11.

Barr, I.D., Spagnolo, M., 2013. Paleoglacial and Paleoclimatic conditions in the NW Pacific, as revealed by a morphometric analysis of cirques on the Kamchatka Peninsula. Geomorphology, 192, 15–29.

Berman, D., Alfimov, A., Kuzmina, S., 2011. Invertebrates of the relict steppe ecosystems of Beringia, and the reconstruction of Pleistocene landscapes. Quat. Sci. Rev. 30, 2200–2219.

Bigg, G. R., Clark, C. D., Hughes, A. C. L., 2008. A last glacial ice sheet on the Pacific Russian Coast and catastrophic change arising from coupled ice-volcanic interactions. Earth Planet Sci. Lett., 265, 559-570.

Braithwaite R. J, Raper, S. C. B, Chutko, K., 2006. Accumulation at the equilibrium line altitude of glaciers inferred from a degree–day model and tested against field observations. Annals of Glaciology, 43, 329–334.

Brigham-Grette, J., Gualtieri, L. M., Glushkova, O. Yu., Hamilton, T.D., Mostoller, D., Kotov, A., 2003. Chlorine-36 and ^{14}C chronology support a limited last glacial maximum across central Chutotka, north-eastern Siberia, and no Beringian ice sheet. Quat. Res. 59, 386–398.

Brugger, K.A., 2006. Late Pleistocene climate inferred from the reconstruction of the Taylor River glacier complex, southern Sawatch Range, Colorado. Geomorphology, 75: 318-329.

Budiko, M.I., Borzenkova, I.I., Menzhulin, G.B., Selyakov, K.I., 1992. Expecting changes of regional climate. Izvestiya AN SSSR, Series Geographica, 4, 36-52 (in Russian).

Caissie, B.E., Brigham-Grette, J., Lawrence, K.T., Herbert, T.D., Cook, M.S., 2010. Last Glacial Maximum to Holocene sea surface conditions at Umnak Plateau, Bering Sea, as inferred from diatom, alkenone, and stable isotope records. Paleoceanography 25, PA1206.

Climate data from Klyuchi climate station. http://de.climate-data.org/location/284590/ (checked September 2015)

Climate data from Petropawlowsk Kamtschatski climate station. http://de.climate-data.org/location/1810/ (checked October 2015)

Climate data from Alkatvaam climate station. http://de.climate-data.org/location/284590/ (checked March 2016).

Climate data from Meynypilgyno climate station. http://de.climate-data.org/location/284590/ (checked March 2016).

Dirksen, V., Dirksen, O., Diekmann, B., 2013. Holocene vegetation dynamics and climate change in Kamchatka Peninsula, Russian Far East. Rev. Paleobot. Palynol. 190, 48–65.

Elias, S.A., 2001. Mutual climatic range reconstructions of seasonal temperatures based on Late Pleistocene fossil beetle assemblages in eastern Beringia. Quat. Sci Rev. 20, 77–91.

Elias, S., Crocker, B., 2008. The Bering Land Bridge: a moisture barrier to the dispersal of steppe–tundra biota? Quat. Sci. Rev., 27(27–28), 2473–2483. http://doi.org/10.1016/j.quascirev.2008.09.011

Felzer, B., 2001. Climate impacts of an ice sheet in East Siberia during the Last Glacial Maximum. Quat. Sci. Rev. 20, 437–447.

Gebhardt, H., M. Sarnthein, P. M. Grootes, T. Kiefer, H. Kuehn, F. Schmieder, U. Röhl, (2008), Paleonutrient and productivity records from the subarctic North Pacific for Pleistocene glacial terminations I to V. Paleoceanography, 23, PA4212 doi:10.1029/2007PA001513.

Glushkova, O. Yu., 2001. Geomorphological correlation of Late Pleistocene glacial complexes of Western and Eastern Beringia. Quat. Sci. Rev. 20, 405–417.

Grosswald MG. 1988. An Antarctic-style ice sheet in the Northern Hemisphere: towards a new global glacial theory. Polar Geography and Geology, 12, 239–267.

Grosswald, M. G.1998. Late Weichselian ice sheets in Arctic and Pacific Siberia. Quat. Int. 45/46, 3–18.

Grosswald, M. G., Hughes, T.J., 2002. The Russian component of an Arctic Ice Sheet during the Last Glacial Maximum. Quat. Sci. Rev. 21, 121–146.

Grosswald, M. G., Hughes, T.J., 2005. "Back-arc" marine ice sheet in the Sea of Okhotsk. Rus. J. Earth. Sci. 7. doi:10.2205/2005ES000180.

Grosswald, M. G., Kotlyakov, V. M., 1969. Present-day glaciers in USSR and some data on their mass balance. J. Glaciol. 8, 9-21.

Gualtieri, L., Glushkova, O., Brigham-Grette, O. J., 2000. Evidence for restricted ice extent during the last glacial maximum in the Koryak Mountains of Chukotka, far eastern Russia. Geol. Soc. Amer. Bull. 112, 1106–1118.

Gualtieri, L., Vartanyan, S., Brigham-Grette, J., Patricia, M., Anderson, P.M., 2003. Pleistocene raised marine deposits on Wrangel Island, NE Siberia: implications for Arctic ice sheet history. Quat. Res. 59, 399–410.

Guthrie, R. D., 2001. Origin and causes of the mammoth steppe: a story of cloud cover, woolly mammal tooth pits, buckles, and inside-out Beringia. Quat. Sci. Rev., 20, 549–574.

Harada, N., Sato, M., Seki, O., Timmermann, A., Moossen, H., Bendle, J., Nakamura, Y., Kimoto, K., Okazaki, Y., Nagashima, K., Gorbarenko, S. a., Ijiri, A., Nakatsuka, T., Menviel, L., Chikamoto, M.O., Abe-Ouchi, A., Schouten, S., 2012. Sea surface temperature changes in the Okhotsk Sea and adjacent North Pacific during the last glacial maximum and deglaciation. Deep Sea Res. Part II Top. Stud. Oceanogr. 61-64, 93–105.

Hughes, P. D. (2008). Response of a Montenegro glacier to extreme summer heatwaves in 2003 and 2007. Geografiska Annaler, Series A, 90(4), 259-267. DOI: 10.1111/j.1468-0459.2008.00344.x.

Hughes, P. D., 2009. Loch Lomond Stadial (Younger Dryas) glaciers and climate in Wales. Geol. J., 44, 375–391.

Hughes, P. D., and Braithwaite, R. J., 2008. Application of a degree-day model to reconstruct Pleistocene glacial climates. Quat. Res. 69, 110–116.

Ivanov, A., 2002. The Far East. In: The Physical Geography of Northern Eurasia, Shahgedanova M. (ed.). Oxford University Press: Oxford, 422-447.

Jones, V., and Solomina, O., 2015. The geography of Kamchatka. Glob. Plan. Change, 134, 3-9.

Kern, Z., László, P., 2010. Size specific steady-state accumulation-area ratio: an improvement for equilibrium-line estimation of small palaeoglaciers. Quat. Sci. Rev. 29, 2781–2787.

Kienast, F., Schirrmeister, L., Siegert, K., Tarasov., P., 2005. Paleobotanical evidence for warm summers in the East Siberian Arctic during the last cold stage. Quat. Res. 63, 283-300.

Kim, S.-J., Crowley, T. J., Erickson, D. J., Govindasami, B., Duffy, P. B., Lee, B. Y., 2008. High-resolution climate simulation of the last glacial maximum. Clim. Dyn., 31, 1-16.

Kuzmina, S. A., Sher, A. V., Edwards, M. E., Haile, J., Yan, E. V., Kotov, A. V., & Willerslev, E. (2011). The late Pleistocene environment of the Eastern West Beringia based on the principal section at the Main River, Chukotka. Quat. Sci. Rev., 30, 2091–2106. http://doi.org/10.1016/j.quascirev.2010.03.019

Laukhin, S. A., Zhimin, J., Pushkar, V. S., Cherepanova, M. V., 2006. Last Glaciation in the northern part of the Eastern Chukchi Peninsula and paleoceanography of the North Pacific. Dokl. Earth Sci., 441A, 1422-1426.

Laumann, T., Reeh, N., 1993. Sensitivity to climate change of the mass balance of glaciers in southern Norway. Journal of Glaciology 39, 656–665.

Lozhkin, A. V., Anderson, P. M., Matrosova, T. V., Minyuk, P. S., 2007. The pollen record from El'gygytgyn Lake: Implications for vegetation and climate histories of northern

Chukotka since the late middle Pleistocene. J Paleolimnol, 37(1), 135–153. http://doi.org/10.1007/s10933-006-9018-5

Lozhkin, A. V., Anderson, P. M., 2013. Late Quaternary records from the Anadyr Lowland, central Chukotka (Russia). Quat. Sci. Rev., 68, 1-16.

Lynch, C., Barr, I.D., Mullan, D., Ruffell, A., 2016. Rapid glacial retreat on the Kamchatka Peninsula during the early 21st Century. The Cryosphere 10, 1809–1821.

Marrero, S.M., Phillips, F.M., Borchers, B., Lifton, N., Aumer, R., Balco, G., 2016. Cosmogenic nuclide systematics and the CRONUScalc program. Quaternary Geochronology 31, 160–187.

Melekestsev, I.V., Braitseva, O. A, Kraevaya, T.S.,1970. Application of the complex techniques to determine the age of Quaternary volcanic formations (in the case of Kamchatka). Izv AN SSSR Set Geol. 10, 149-153 (in Russian).

Meyer, H., Dereviagin, A., Siegert, C., Hubberten, H.-W., 2002. Paleoclimate studies on Bykovsky Peninsula, North Siberia - hydrogen and oxygen isotopes in ground ice. Polarforschung 70, 37–51.

Meyer, V. D., Lohmann, G., Hefter, J., Tiedemann, R., Mollenhauer, G., 2016 a. Development of summer temperature on the Kamchatka Peninsula, Russian Far East, over the past 20,000 years. Clim. Past Discuss., doi:10.5194/cp-2016-21, in review.

Meyer, V. D., Max, L., Hefter, J., Tiedemann, R., Mollenhauer, G., 2016 b. Glacial-to-Holocene evolution of sea surface temperature and surface circulation in the subarctic Northwest Pacific and the Western Bering Sea. Paleoceanography 31, 916-927, doi:10.1002/2015PA002877.

Mix, A. C., Bard, E., Schneider, R., 2001. Environmental processes of the ice age: land, ocean, glaciers (ELIPOG). Quat. Sci. Rev., 20, 627-657.

Mock, C.J., Mock, C.J., Bartlein, P.J., Bartlein, P.J., Anderson, P. A, Anderson, P. A, 1998. Atmospheric circulation patterns and spatial climatic variations. Beringia. Int. J. Climatol. 10, 1085–1104.

Reimer, P.J., Bard, E., Bayliss, A., Beck, J.W., Blackwell, P.G., Bronk Ramsey, C., Buck, C.E., Cheng, H., Edwards, R.L., Friedrich, M., Grootes, P.M., 2013. IntCal13 and Marine13 radiocarbon age calibration curves 0-50,000 years cal BP. Radiocarbon 55(4), 1869–1887.

Ohmura A, Kasser P, Funk M. 1992. Climate at the equilibrium line of glaciers. Journal of Glaciology 3, 397–411.

Sakamoto, T., Ikehara, M., Aoki, K., Iijima, K., Kimura, N., Nakatsuka, T., Wakatsuchi, M., 2005. Ice-rafted debris (IRD)-based sea-ice expansion events during the past 100 kyrs in the Okhotsk Sea. Deep Sea Res. Part II 52 (16-18), 2275-2301.

Sancetta, C., 1983. Effect of Pleistocene glaciation upon oceanographic characteristics of the North Pacific Ocean and the Bering Sea. Deep Sea Res., 30, 851-869.

Seki, O., Bendle, A. J., Harada, N., Kobayashi, N. Sawada, K., Moossen, H., Inglis, G. N., Nagao, S., Sakamoto, T., 2014. Assessment and calibration of TEX_{86} paleothermometry in the Sea of Okhotsk and the sub-polar North Pacific region: Implications for paleoceanography. Progr. Oceanogr., 126, 254-266.

Seki, O., Kawamura, K., Ikehara, M., Nakatsuka, T., Oba, T., 2004. Variation of alkenone sea surface temperature in the Sea of Okhotsk over the last 85 kyrs. Org. Geochem., 35, 347-354.

Seki. O., Sakamoto, T., Saki, S., Schouten, S., Hopmans, E., C., Sinninghé Damsté, J. S., Pancost, R. D., 2009. Large changes in sea ice distribution and productivity in the Sea of Okhotsk during the deglaciations. Geochem., Geophys., Geosyst., 10, Q10007.

Sergin, S. Ya., Scheglova, M.S., 1976. Beringia climate during ice ages as result of influence of global and local factors. In: Beringia in the Cenozoic. Nauka Press, Vladivostok, pp. 171-175 (in Russian).

Siegert, M.J., Dowdeswell, J.A., Hald, M., Svendsen, J., 2001. Modelling the Eurasian Ice Sheet through a full (Weichselian) glacial cycle. Global Planet. Change 31, 367–385.

Shahgedanova M., Perov, V., Mudriv, Y. 2002. In: The Physical Geography of Northern Eurasia, Shahgedanova M. (ed.). Oxford University Press: Oxford, 284-313.

Sher, A. V., Kuzmina, S. A., Kuznetsova, T. V. and Sulerzhitsky, L. D., 2005. New insights into the Weichselian environment and climate of the East Siberian Arctic, derived from fossil insects, plants, and mammals, Quat. Sci. Rev., 24(5-6), 533–569, doi:10.1016/j.quascirev.2004.09.007.

Small, D., Clark, C.D., Chiverrell, R.C., Smedley, R.K., Bateman, M.D., Duller, G.A.T., Ely, J.C., Fabel, D., Medialdea, A., Moreton, S.G., 2016. Devising quality assurance procedures for assessment of legacy geochronological data relating to deglaciation of the last British-Irish Ice Sheet. Earth-Science Reviews, in press. doi:10.1016/j.earscirev.2016.11.007.

Smirnova, M. A., Kazarina, G. K., Matul, A. G. and Max, L., 2007. Diatom Evidence for Paleoclimate Changes in the Northwestern Pacific during the Last 20000 Years, Mar. Geol. 55(3), 425–431, doi:10.1134/S0001437015030157.

Solomina, O., Calkin, P., 2003. Lichenometry as applied to moraines in Alaska, USA, and Kamchatka, Russia. Arct., Antarc., Apl. Res., 35, 129-143.

St. John, K.E., Krissek, L.A., 1999. Regional patterns of Pleistocene ice-rafted debris flux in the North Pacific. Paleoceanography 14, 653–662.

Stauch, G., and Gualteri, L., 2008. Late Quaternary Glaciations in northeastern Russia. J.Quat. Sci., 23, 6-7.

Stauch, G., Lehmkuhl, F., 2010. Quaternary glaciations in the Verkhoyansk Mountains, Northeast Siberia. Quaternary Research 74, 145-155.

Stuiver, M., Reimer, P.J., Reimer, R.W., 2016. CALIB 7.1 [WWW program]. http://calib.org, (accessed: 10.12.16).

Velichko, A. A., 1993. North Eurasian landscape and climate development. The Late Pleistocene/Holocene: Elements of Forecast. Iss. I. Regional Paleogeography. Nauka Press, Moscow (in Russian).

Velichko, A.A., Wright, H.E., Barnosky, C.W., 1984. Late Quaternary Environments of the Soviet Union, University of Minnesota Press, Minneapolis.

Yanase, W. and Abe-Ouchi, A.: The LGM surface climate and atmospheric circulation over East Asia and the North Pacific in the PMIP2 coupled model simulations, Clim. Past, 3(3), 439–451, doi:10.5194/cp-3-439-2007.

Zech, W., Zech, R., Zech, M., Leiber, K., Dippold, M., Frechen, M., Bussert, R., Andreev, A., 2011. Obliquity forcing of Quaternary glaciation and environmental changes in NE Siberia. Quaternary International 234, 133-145.

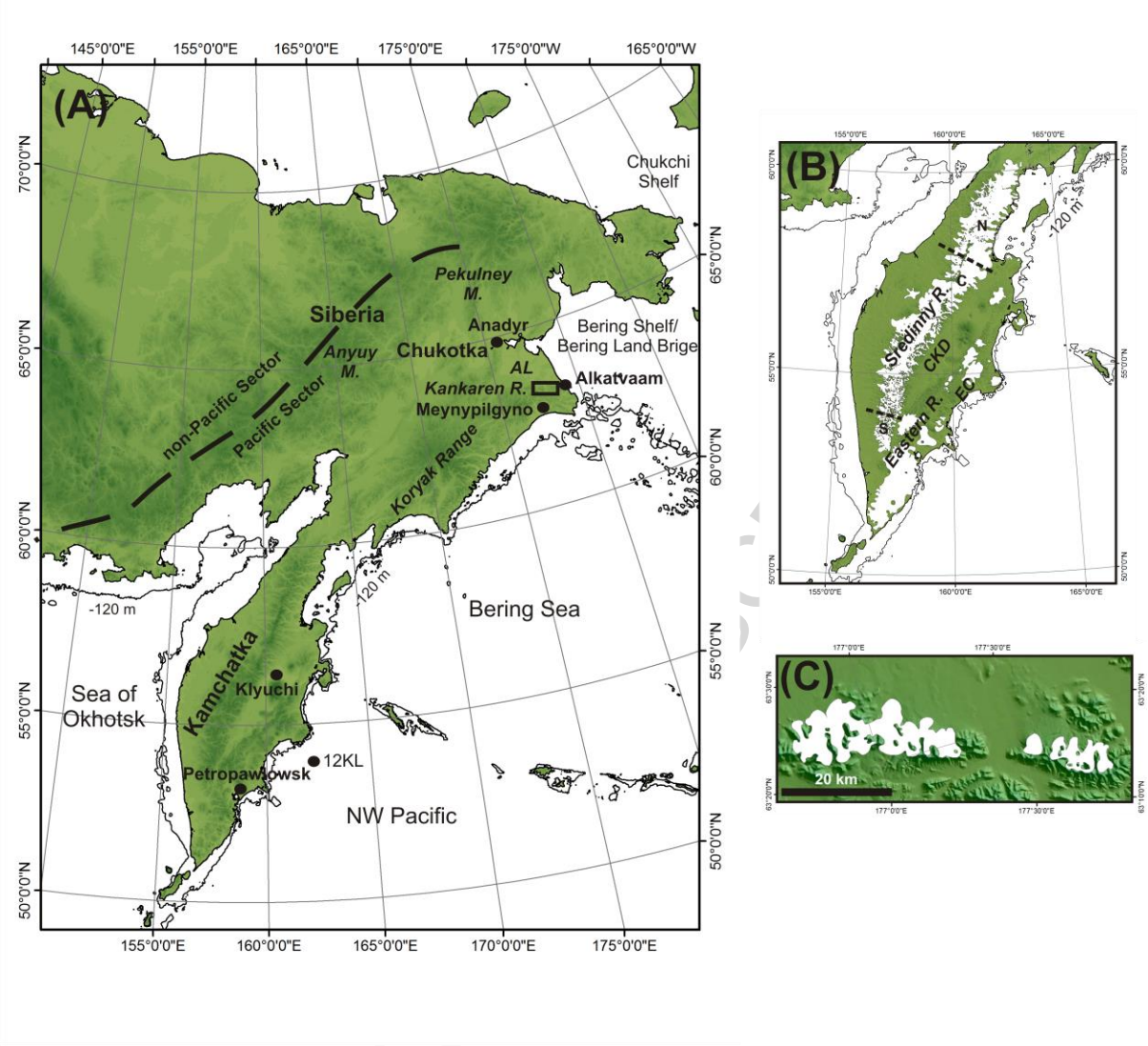

Figure 1

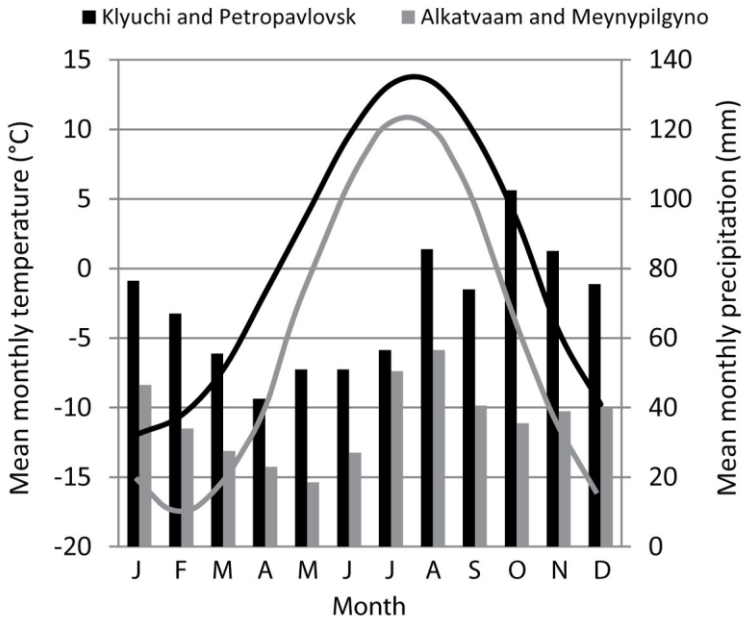

Figure 2

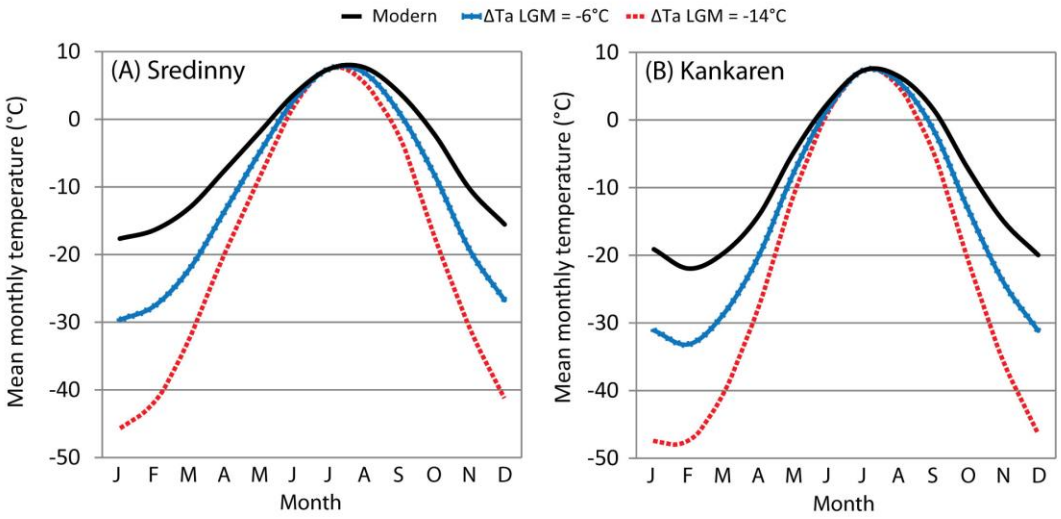

Figure 3

Figure captions:

Figure 1. (A) Overview of Northeast Russia showing the regions mentioned in the text. The division into Pacific and non-Pacific sectors (dashed line) is based upon Grosswald and Kotlyakov (1969). The gLGM shore line is sketched (solid line, sea-level ~ 120 m below present). The rectangle marks the position of the Kankaren Range. Black dots indicate sites mentioned in the text. M: Mountains; R: Range; AL: Anadyr Lowland. (B) Glacier reconstruction in the Sredinny Range and the Eastern Range for the gLGM (24-18 ka BP) after Barr and Clark (2011) and Barr and Solomina (2014) and references therein. Dashed lines indicate the different sectors of the Sredinny ice field. N: northern sector, C: central sector, S: southern sector. EC: Eastern Coast; CKD: Central Kamchatka Depression; (C) Reconstructed glaciation in the Kankaren Range during the gLGM after Barr and Clark (2011).

Figure 2. Modern climate data averaged for stations in Klyuchi and Petropavlovsk (for Kamchatka/the Sredinny Range), and Alkatvaam and Meynypilgyno (for the Kankaren Range). These data were taken from (http://en.climate-data.org) and are corrected to sea level using a lapse-rate of 0.63°C/100 m.

Figure 3. Modern and modelled LGM temperatures at the ELAs of LGM glaciers in (A) the Sredinny (ELA = 897 m.a.s.l.) and (B) Kankaren (ELA = 575 m.a.s.l.) mountain ranges (ELA estimates based on Barr and Clark, 2011). Modern climate data (plotted in black) is derived from climate stations in Klyuchi and Petropavlovsk (for the Sredinny Range), and Alkatvaam and Meynypilgyno (for the Kankaren Range), and is corrected to the LGM ELAs using a lapse-rate of 0.63°C/100 m. Climate conditions at the LGM are modelled assuming perturbations in mean annual temperature ($\Delta T_{a\ LGM}$) of -6°C and -14°C, as predicted by the climate model of Kim et al. (2008).

Table 1

Modern at s. l.	Sredinny Range	Kankaren Range
T_{July}[°C]	13.3	10.9
T_a [°C]	0.6	-5.1
A_y[°C]	12.7	16.0

Table 2

		Sredinny Range								Kankaren Range	
LGM conditions at ELA	Average ELA [m.a.s.l.]	1035 (south)	876 (centre)	808 (north)	897 (mean)	1035 (south)	876 (centre)	808 (north)	897 (mean)	575 (mean)	
	DDF (mm d^{-1} $°C^{-1}$)	4.0	4.0	4.0	4.0	4.0	4.0	4.0	4.0	4.0	4.0
	$T_{July\ LGM}$ [1]	6.7	7.7	8.2	7.6	6.7	7.5	8.2	7.6	7.2	7.2
	$\Delta T_{a\ LGM}$ [°C]	**-6.0**	**-6.0**	**-6.0**	**-6.0**	**-14.0**	**-14.0**	**-14.0**	**-14.0**	**-6.0**	**-14.0**
	$A_{y\ LGM}$ [°C]	**18.6**	**18.6**	**18.6**	**18.6**	**26.6**	**26.6**	**26.6**	**26.6**	**22.0**	**30.0**
	$T_{a\ LGM}$ [°C]	-11.9	-11.1	-10.5	-11.1	-19.9	-19.1	-18.5	-19.0	-14.6	-22.7
	Ablation [days]	102	110	113	108	84	90	93	90	88	71
	Annual prec. [mm yr^{-1}]	1780	2203	2394	2145	1479	1829	1986	1781	1291	943
	Prec. change relative to modern [%] [2]	+18.7 + 48.8	+46.8 +83.6	+59.6 +99.5	+43.0 +78.8	-1.4 +23.3	+21.9 +52.4	+32.4 +65.5	+18.7 ± 48.4	n.a. [3]	n.a. [3]

[1]: calculated from modern T_{July} (Table 1) using a lapse rate of 0.0063°C/m

[2]: first value refers to 1500 mm yr^{-1}, the second to 1200 mm yr^{-1}.

[3]: cannot be estimated since modern precipitation data for the mountains are not available (n.a.).

Table 3

		Sredinny Range								Kankaren Range	
LGM conditions at ELA	Average ELA [m.a.s.l.]	1035 (south)	876 (centre)	808 (north)	897 (mean)	1035 (south)	876 (centre)	808 (north)	897 (mean)	575 (mean)	575 (mean)
	DDF (mm d^{-1} °C^{-1})	2.5	2.5	2.5	2.5	2.5	2.5	2.5	2.5	2.5	2.5
	$T_{July\ LGM}$[1]	6.7	7.7	8.2	7.6	6.7	7.5	8.2	7.6	7.2	7.2
	$\Delta T_{a\ LGM}$ [°C]	**-6.0**	**-6.0**	**-6.0**	**-6.0**	**-14.0**	**-14.0**	**-14.0**	**-14.0**	**-6.0**	**-14.0**
	$A_{y\ LGM}$ [°C]	**18.6**	**18.6**	**18.6**	**18.6**	**26.6**	**26.6**	**26.6**	**26.6**	**22.0**	**30.0**
	$T_{a\ LGM}$ [°C]	-11.9	-10.9	-10.5	-11.0	-19.9	-18.9	-18.5	-19.0	-14.7	-22.7
	Ablation [days]	102	110	113	108	84	90	93	90	88	71
	Annual prec. [mm yr^{-1}]	1112	1377	1496	1340	924	1143	1241	1113	807	589
	Prec. change relative to modern [%] [2]	-25.8 -7.3	-8.2 +14.8	-0.2 +24.6	-10.6 +11.7	-38.4 -23.0	-23.8 -4.8	-17.3 +3.4	-25.8 -7.3	n.a.[3]	n.a.[3]

[1]: calculated from modern T_{July} (Table 1) using a lapse rate of 0.0063°C/m

[2]: first value refers to 1500 mm yr^{-1}, the second to 1200 mm yr^{-1}.

[3]: cannot be estimated since modern precipitation data for the mountains are not available (n.a.).

Table caption

Table 1. Modern mean July and annual temperatures and amplitudes of the annual temperature cycle in Kamchatka and the Kankaren area. The data were taken from Klyuchi and Petropawlowsk (Sredinny Range) and Alkatvaam and Meynypilgyno climate stations (Kankaren Range) and were corrected to sea level using a lapse-rate of 0.0063°C/m.

Table 2. DDM temperature-setup for the LGM simulations and results for precipitation (prec.) and the length of the ablation season. The model was run with $\Delta T_{a\ LGM}$ values based on climate-model estimates from Kim et al. (2008), and with a degree-day melt factor (DDF) of 4.0 (describing temperate glaciers) assuming that LGM T_{July} was the same as at present. Percentage change relative to modern is calculated using modern precipitation estimates of 1200 mm yr^{-1}–1500 mm yr^{-1} (for the Sredinny Range).

Table 3. DDM temperature-setup for the LGM simulations and results for precipitation (prec.) and the length of the ablation season. The model was run with $\Delta T_{a\ LGM}$ values based on climate-model estimates from Kim et al. (2008), and with a degree-day melt factor (DDF) of 2.5 (describing glaciers of polar type) assuming that LGM T_{July} was the same as at present. Percentage change relative to modern is calculated using modern precipitation estimates of 1200 mm yr^{-1}–1500 mm yr^{-1} (for the Sredinny Range).

Highlights to the manuscript:

Linking glacier extent and summer temperature in NE Russia - implications for precipitation during the global Last Glacial Maximum

1) Precipitation in SE Siberia at the gLGM is inferred from glacier mass balance
2) Summers as warm as today are assumed based on proxy data
3) In Pacific Siberia annual precipitation equaled or exceeded modern
4) Pacific Siberian summer warmth rather than aridity limited glaciation at the gLGM